Elastic scattering and fusion of $^{16}O+^{59}Co$ at near barrier energies: A signature for long range fusion potentials

C. Tenreiro,* P. R. S. Gomes,† T. J. P. Penna,† R. Liguori Neto, J. C. Acquadro, P. A. B. Freitas, and E. Crema
Instituto de Física, Universidade de São Paulo, Laboratorio Pelletron,
Caixa Postal 20516 São Paulo, 01452-990 São Paulo, Brazil
(Received 27 July 1993)

Elastic scattering angular distributions were measured for the $^{16}O+^{59}Co$ system, at energies close to the Coulomb barrier. Simultaneous analysis of elastic scattering and fusion cross sections were performed, based on the optical model. The part of the imaginary potential which accounts for the fusion was found to be of long range, with values of r_f larger than 1.42 fm, leading to the interpretation that fusion is decided at large separations, beyond the Coulomb barrier.

PACS number(s): 25.70.Bc, 25.70.Jj, 24.10.Ht

Fusion cross sections have been measured by our group for the $^{16}O+^{59}O$ system [1,2] at near and sub-barrier energies. The large enhancement of the experimental sub-barrier fusion cross section, when compared with the predictions of any one-dimensional barrier penetration model (BPM), could not be explained either by the Wong model or by the inelastic coupled channels calculations. Both approaches lead to very small fusion enhancement. Only with the additional coupling of transfer channels could the fusion data be fitted, within the uncertainties of the simplified coupled channels, analysis and the values of the derived transfer form factors.

From that analysis [2] one has concluded that the fusion process might start to occur at a large separation of the colliding nuclei, even before the Coulomb barrier is penetrated. The stripping of one alpha particle channel was found to be mainly responsible, when coupled to the fusion, for the large sub-barrier fusion cross section enhancement. As its transfer cross section to excited states was below the measurable level [1,2], one has interpreted it as a virtual channel acting as a doorway to fusion. From a semiclassical formalism [3], it was derived [2] that the average transfer distance for this channel is relatively small, $\langle d_{\rm tr}\rangle = 1.59$ fm, not far from the position of the Coulomb barrier (1.48 fm), its form factor is very steep, and the effective Q value is positive. From a macroscopic approach, the fusion cross section for this system could be explained [2] by the liquid drop model suggested by Aguiar *et al.* [4], where a neck coordinate is introduced. The neck formation process has the effect of increasing the distance of no return from fusion. One has learned in the last years that reaction mechanisms, at near barrier energies, increase in complexity when they take place at small distances, because quasielastic channels couple strongly to the elastic channel and to each other, and play the role of a doorway to more complex and dissipative processes, such as the fusion. It is, therefore, quite important to study the distances where the reaction process take place, in order to understand the interplay between them.

As we had the above-mentioned indications, for the $^{16}O+^{59}Co$ system, leading to the same predictions of the direct reaction formalism developed by Udagawa, Kim, and Tamura [5,6], where a long range fusion absorptive potential is derived, we decided to apply this formalism to the simultaneous analysis of the fusion and elastic scattering data for this system, in order to investigate the compatibility of the results by different approaches.

Elastic scattering angular distribution data were available in the literature [7] in the energy range $36 \le E_{\rm lab} \le 56$ MeV and $20° \le \theta_{\rm c.m.} \le 180°$. We have obtained new data for $37 \le E_{\rm lab} \le 62$ MeV and angular distributions within the range $20° \le \theta_{\rm c.m.} < 180°$. For the low energy region, from 37 to 42 MeV, the data were taken at 0.5 MeV steps of the bombarding energy. In this region the imaginary part of the optical potential decreases rapidly as the energy goes down. The experiments were performed at the São Paulo Pelletron Laboratory, using an array of nine silicon surface barrier detectors, with energy resolution of the order of 300 keV. The inelastic yield was found to be very small, in agreement with the results obtained by the in-beam gamma ray spectroscopy method [1,2].

In the direct reaction formalism [5,6], the fusion cross section is calculated as

$$\sigma_f = \frac{2}{\hbar v_a}\langle \chi_a^{(+)}|W_f(r)|\chi_a^{(+)}\rangle \ ,$$

where W_f is the part of the imaginary potential W_a which accounts for the absorption into the fusion channel. In this expression v_a is the incident velocity and $\chi_a^{(+)}$ is the elastic scattering wave function calculated from the full optical potential $U_a(r) = -V_a(r) - iW_a(r)$ and determined from the elastic scattering data. The symbol a stands for the elastic scattering channel. The real nuclear potential and W_f have the usual Woods-Saxon form.

The calculations were performed using two different

*Present address: Departamento de Física, Facultad de Ciencias, Universidad de Chile, Casilla 653, Santiago 1, Chile.
†Present address: Departamento de Física, Universidade Federal Fluminense, Out. S. João Batista, Niteroi, RJ 24020, Brazil.

sets of optical potential parameters. One of them was the same set determined by Tannous *et al.* in Ref. [7], from the elastic scattering data, where the geometrical parameters were kept fixed as $r_r = r_i = 1.22$ fm and $a_r = a_i = 0.5$ fm. The second set was obtained assuming an energy dependence of the imaginary potential W_a as [8]

$$W(E) = \frac{1}{1+\exp[(E_b - E)/a_e]} ,$$

where E_b is the energy of the Coulomb barrier (38.8 MeV) and a_e is the diffuseness of the energy dependence (4.6 MeV). The complete energy-dependent real potential was then obtained by using the dispersion relation [8] and assuming a bare potential as a Woods-Saxon type, with a proper normalization in order to get a correct magnitude of V_0. For energies where fusion data were available, but not the elastic scattering data, a smooth variation of the total reaction cross section was assumed.

The next step was to assume that

$$W_f = \begin{cases} W_a, & r \le R_f = r_f(A_1^{1/3} + A_2^{1/3}), \\ 0, & r > R_f . \end{cases}$$

Then the imaginary potential was cut off at R_f and assumed to be the fusion absorptive potential, with r_f as the only free parameter. The fusion cross section is now written as

$$\sigma_f = \frac{\pi}{k_a^2} \sum_{l_a=0}^{\infty} (2l_a + 1) T_{f,l_a} ,$$

where

$$T_{f,l_a} = \frac{4}{\hbar v_a} \int_0^{R_f} |\chi_{l_a}(r)|^2 W_a(r) dr .$$

The fusion cross section defined by these expressions is called the elastic fusion cross section, and it includes fusion processes which may proceed into some direct reaction channels before reaching the fused state. The code FRESCO [9] was used in order to calculate σ_f.

For the whole energy region studied, the values of r_f which fit the experimental fusion data are in the range of 1.47 ± 0.05 fm, increasing as the energy decreases. (The reduced Coulomb barrier radius for the system is 1.48 fm.) This range of r_f seems to be a general trend, since it was also obtained in the analysis of heavier systems [10,11]. The dotted line in Fig. 1 shows the fit of the fusion data by this procedure. The solid line shows the fit when the parameter r_f is kept fixed at 1.45 fm, which is its value at $E_{lab} = 40$ MeV, the reference energy at which both fusion and elastic scattering data were available. The dashed line is the result of the prediction of the fusion cross section using an one-dimensional barrier penetration model [12].

A long range fusion potential is, therefore, compatible with the interpretation that neck formation leading to fusion can occur at large distances and also that transfer reactions which take place at relatively small distances proceed along a chain of increasing complexity, acting as a multistep process leading to fusion. From the three approaches, one finds that the point of no return from

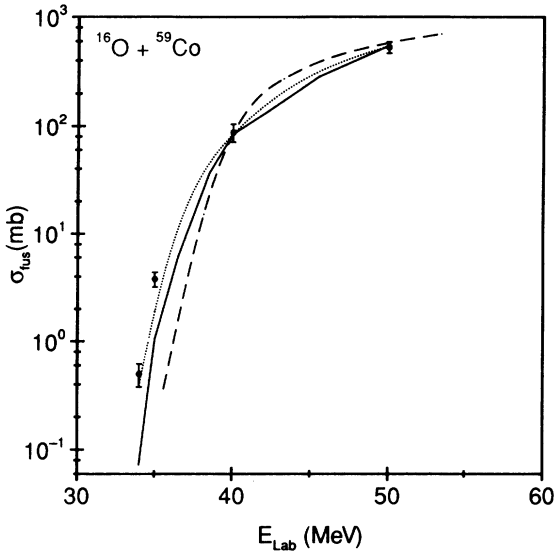

FIG. 1. Fits of the fusion excitation function: dashed line, prediction of the one-dimensional barrier penetration model (KNS); solid line, obtained for a fixed value of $r_f = 1.45$ fm; dotted line, best fit for values of r_f varying within the range 1.47 ± 0.05 fm.

fusion is reached at distances beyond the position of the Coulomb barrier. Figure 2 shows, schematically, the evolution of the reaction process as a function of the separation distance of the two colliding nuclei. Absorption starts to occur at $d_a = 1.74$ fm [2], when simple quasielastic processes take place. From $r_f = 1.52$ fm up to the position of the Coulomb barrier, $r_b = 1.48$ fm [2], the fusion

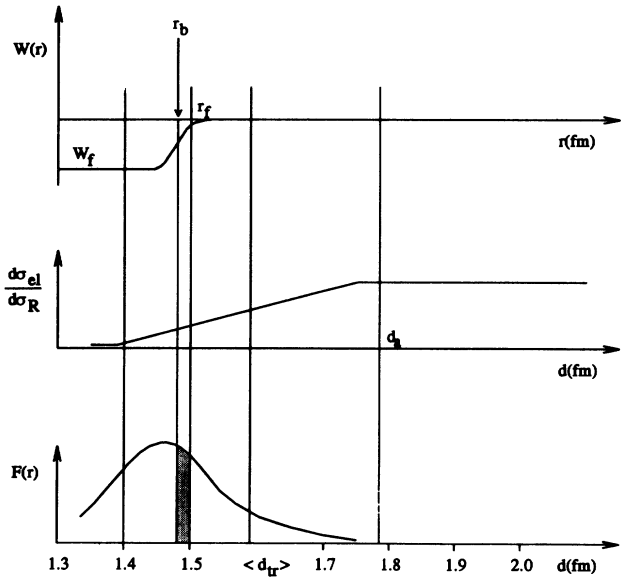

FIG. 2. Scheme of the evolution of the reaction process as a function of the separation distance of the colliding nuclei. At the top, the fusion absorptive potential with range r_f, The central figure shows the absorption from the elastic channel. At the bottom, the transfer form factor for the stripping of one alpha particle. The dark region is where the fusion process occurs before the barrier is penetrated and transfer reactions act as a doorway to fusion.

absorption potential is already present, meaning that the flux leaving the elastic channel leads, in a multistep process, to more complex channels such as fusion; this is the region where the neck formation occurs, and transfer channels couple to fusion and consequently, enhance the fusion cross section.

From the three approaches, one learns that the sub-barrier fusion cross section enhancement may be interpreted as arising not just by the splitting and lowering of the Coulomb barrier relative to the BPM predictions, but also by the additional attraction in the incident channel, as a result of the strong absorption under or even outside the barrier.

[1] P. R. S. Gomes, T. J. P. Penna, R. Liguori Neto, J. C. Acquadro, C. Tenreiro, P. A. B. Freitas, E. Crema, N. Carlin Filho, and M. M. Coimbra, Nucl. Instrum. Methods A **280**, 395 (1989).

[2] P. R. S. Gomes, T. J. P. Pena, E. G. Chagas, R. Liguori Neto, J. C. Acquadro, P. R. Pascholati, E. Crema, C. Tenreiro, N. Carlin Filho, and M. M. Coimbra, Nucl. Phys. **A534**, 429 (1991).

[3] L. Corradi, S. J. Skorka, K. E. G. Löbner, P. R. Pascholati, U. Quade, K. Rudolph, W. Shomburg, M. Steimayer, H.-G. Thies, G. Montagnoli, D. R. Napoli, A. M. Stefanini, A. Tivelli, S. Beghini, F. Scarlassara, C. Signorini, and F. Soramel, Z. Phys. A **344**, 55 (1990).

[4] C. E. Aguiar, V. C. Barbosa, L. F. Canto, and R. Donangelo, Phys. Lett. B **201**, 22 (1988); Nucl. Phys. **A472**, 571 (1987).

[5] T. Udagawa, T. Kim, and T. Tamura, Phys. Rev. C **32**, 142 (1985).

[6] T. Kim, T. Udagawa, and T. Tamura, Phys. Rev. C **33**, 370 (1986).

[7] N. B. J. Tannous, J. F. Mateja, D. C. Wilson, L. R. Modsker, and R. H. Davis, Phys. Rev. C **18**, 2190 (1978).

[8] C. Mahaux, H. Ngo, and G. R. Satchler, Nucl. Phys. **A449**, 354 (1986).

[9] I. J. Thompson, Comput. Phys. Rep. **7**, 167 (1988).

[10] T. Udagawa, T. Tamura, and T. Kim, Phys. Rev. C **39**, 1840 (1989).

[11] H. L. Halbert, J. R. Beene, D. C. Hensley, K. Hokanen, T. M. Semkow, V. Abenante, D. Sarantites, and Z. Li, Phys. Rev. C **40**, 2558 (1989).

[12] A. J. Krappe, J. R. Niz, and A. Sierk, Phys. Rev. C **20**, 992 (1979).

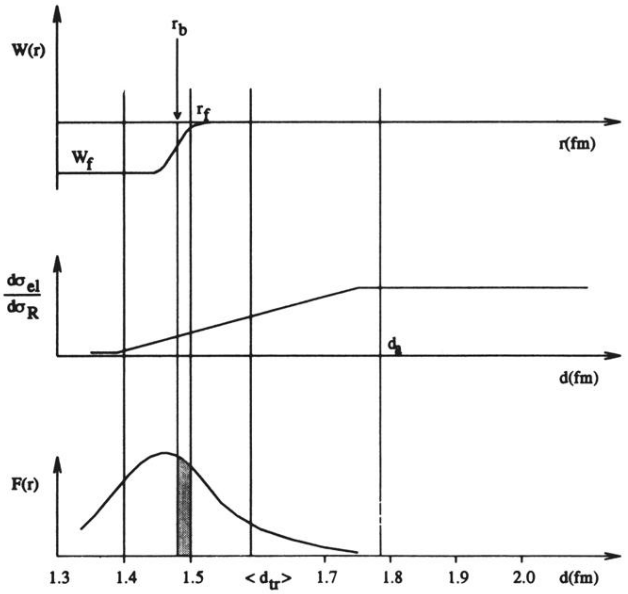

FIG. 2. Scheme of the evolution of the reaction process as a function of the separation distance of the colliding nuclei. At the top, the fusion absorptive potential with range r_f, The central figure shows the absorption from the elastic channel. At the bottom, the transfer form factor for the stripping of one alpha particle. The dark region is where the fusion process occurs before the barrier is penetrated and transfer reactions act as a doorway to fusion.